J. Phys. Chem. A **2003,** *107,* 3497−3502

Photodissociation of SO_2 Clusters[†]

S. M. Hurley, T. E. Dermota, D. P. Hydutsky, and A. W. Castleman, Jr.*

Departments of Chemistry and Physics, The Pennsylvania State University, University Park, Pennsylvania 16802

Received: September 18, 2002; In Final Form: December 17, 2002

Clusters of SO_2 have been interrogated using pump−probe spectroscopy employing a femtosecond laser system coupled to a reflectron time-of-flight mass spectrometer. Upon excitation of the C state of SO_2 with 397.5 nm light and 399.0 nm light, it was found that the photodissociation of SO_2 clusters involves multiple reaction pathways. A mechanism is proposed where the excited cluster either follows a simple exponential decay corresponding to the dissociation of the excited moiety directly from the C state or, alternatively, the excited cluster first fragments and then the excited molecule proceeds through the dissociation process associated with the C state.

Introduction

In the atmosphere, the oxidation of SO_2 ultimately yields H_2SO_4. H_2SO_4 is an important constituent of acid rain and is also found in the aerosol layer present in the lower stratosphere, which plays a role in the radiation balance. Due to its potential importance in the chemistry of the atmosphere, it is of interest to study the photochemistry of SO_2 and its clusters. Several studies have been devoted to an investigation of the spectroscopy and photodissociation of SO_2 from the C ($2\,^1A'$) state, which was found to involve predissociation to the lower repulsive states.[1,2] Sato and co-workers looked at the two-photon dissociation of the B state over the wavelength range 286−309 nm.[3] Computations of the potential energy surfaces of the $X(^1A_1)$ and $C(^1B_2)$ electronic states were performed by Nachtigall et al. to study the photodissociation pathway by means of high level ab initio methods.[4] In a recent study of the dynamics of the E state, Wisniewski et al. determined the lifetime of this excited state to be 271 ± 8 fs.[5] Only a relatively few studies have been reported for SO_2 clusters.[6,7] Zhong et al. have studied the metastable decay of SO_2 clusters and mixed clusters of SO_2 with water and determined the core structure of cluster cations.[8] When clusters of SO_2 undergo photoionization, several reaction channels are possible:

$$(SO_2)_n + h\nu \rightarrow (SO_2)_n^{\ +} + e^- \tag{1}$$

$$\rightarrow [SO(SO_2)_{n-1}]^+ + O + e^- \tag{2}$$

$$\rightarrow [S(SO_2)_{n-1}]^+ + 2O + e^- \tag{3}$$

Despite the wealth of information regarding this system, knowledge of the dynamics of the reactions of SO_2 clusters is lacking. In this paper, a study of the dynamics of SO_2 clusters excited to the C ($2\,^1A'$) state is reported. Evidence is presented that supports a mechanism of dissociation of SO_2 clusters from the C state by multiple pathways.

Experimental Methods

A reflectron time-of-flight mass spectrometer (RETOF-MS) and femtosecond laser system coupled with the pump−probe technique[9] has been utilized to study the dynamics of SO_2. Clusters were formed by supersonic expansion of a 10% mixture of SO_2 (Matheson Gas) in argon with a total backing pressure of about 3 bar. The laser system used in these experiments consists of a mode-locked Ti:sapphire oscillator (Spectra Physics Tsunami) pumped by a 10 W argon ion laser (Spectra Physics 2060), which generates an 82 MHz pulse train.[10−12] Pulse amplification is carried out with a regenerative Ti:sapphire amplifier pumped by the second harmonic of a 10 Hz Nd:YAG laser (Spectra Physics GCR 150−10). Typical output from the amplifier is a beam with a wavelength centered around 795 nm, having a pulse width of 100 fs and a pulse energy of about 3 mJ. In the present study, the fundamental wavelength was frequency doubled with a BBO crystal to generate the second harmonic, which was used as the pump beam. The fundamental wavelength (∼795 nm) was utilized as the probe beam.

Results

A typical mass spectrum is shown in Figure 1, which contains peaks corresponding to the dissociation products shown in eqs 1 and 2. Products associated with eq 3 are not observed in these experiments, but peaks corresponding to masses 16 and 32 amu are observed. These have been assigned as $^{16}O^+$ and $^{32}S^+$, respectively. On the basis of the isotope abundance of atomic sulfur, the peak at 32 amu was determined to be $^{32}S^+$ and not $^{16}O_2^{\ +}$. A trace amount of acetone, which has been extensively studied in our laboratory under similar conditions, was added as a calibrant molecule.

Figure 2 shows the pump−probe transient of $SO_2^{\ +}$, pumped with 399.0 nm light. The kinetics of the photodissociation products are modeled with previously established methods[13,14] and based on the proposed reaction mechanism discussed in a later section of the paper. This species exhibits a growth time of 0.064 ps and decay time (τ_d) of 0.505 ps. The thick solid line in Figure 2 represents the best fit of the data points (squares), which is a sum of a Gaussian response near the temporal zero (thin solid line) and the growth/decay dynamics at positive delay times, which is displayed by the thick dashed line. The growth/decay curve is characteristic of the kinetics of a reaction product. Extensive attempts were made to force the growth component of $SO_2^{\ +}$ and SO^+ to zero so that the

---

[†] Part of the special issue "George S. Hammond & Michael Kasha Festschrift".

10.1021/jp022097c CCC: $25.00

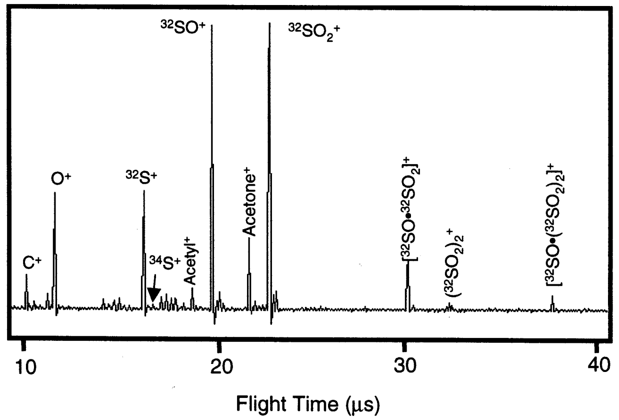

Figure 1. Truncated time-of-flight mass spectrum showing a typical mass distribution of SO_2 cluster fragments and small clusters taken with temporally overlapped 398.0 nm and ~795 nm pump and probe pulses.

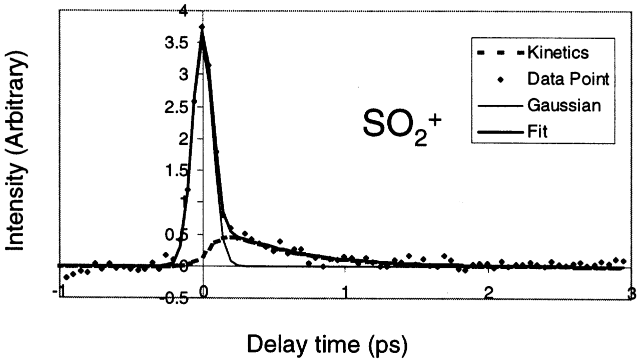

Figure 2. Pump−probe temporal response of SO_2^+ showing a Gaussian response near the temporal overlap followed by a growth (τ_g) and decay (τ_d) of the dynamics at positive delay times. The pump wavelength is 399.0 nm with a pump power of 0.22 mJ and a probe power of 1.0 mJ. (These data are shown again in Figure 4A for comparison.)

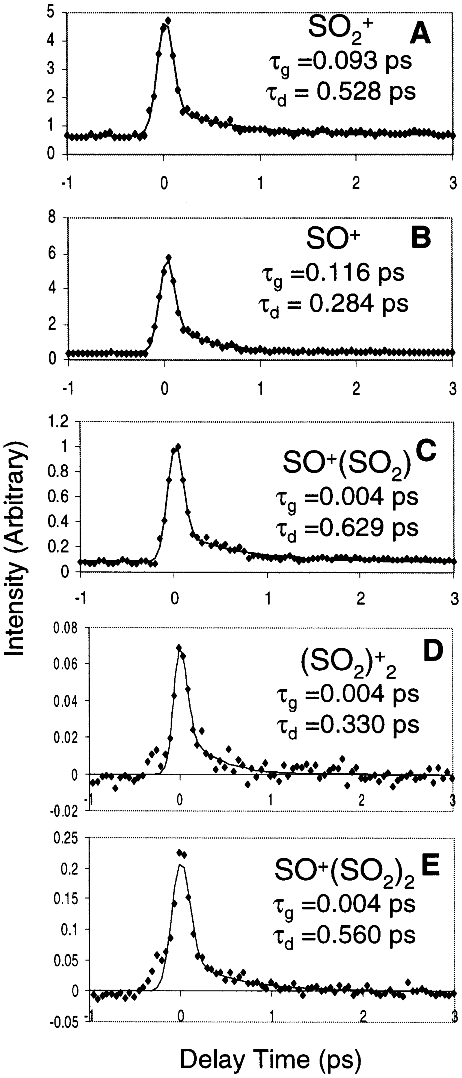

Figure 3. Pump−probe temporal response of SO_2 cluster ions and fragments: (A) SO_2^+; (B) SO^+; (C) $SO^+(SO_2)$; (D) $(SO_2)_2^+$; (E) $SO^+(SO_2)_2$. The solid line represents the best fit of data points (squares). The pump wavelength and power are 397.5 nm and 0.16 mJ, respectively. The probe power is 0.95 mJ. The growth time is given by τ_g, and decay time is given by τ_d.

dynamics would be that of a simple exponential decay. Each attempt resulted in a fitting that was composed of a growth component, indicating that the dynamics is not that of a simple exponential decay and that the growth component is not an artifact of the fitting procedure.

Figure 3 shows the pump−probe transients of dissociation products and clusters pumped with 397.5 nm light. It can be seen that the SO_2^+ (panel A) and SO^+ (panel B) both show growth and decay components in the pump−probe temporal response. The three cluster species shown in Figure 3C−E show a growth time of 0.004 ps. This can be assumed to be zero, which means that these species are not formed in the photodissociation reactions and are thus reactants. In Figure 4, the pump−probe transient dynamics of SO_2 clusters and fragments pumped with 399.0 nm light are shown. The SO_2^+ (panel A) and SO^+ (panel B) both show a growth and decay, indicating that these species are products of the photodissociation. Again, in the case of the cluster species (panels C−E), the growth time can be considered zero; thus the cluster species are reactants and their dynamics follow a simple exponential decay. As noted, the data shown in Figures 3 and 4 were collected at slightly different wavelengths, 397.5 and 399.0 nm, respectively. A comparison of the two sets of data shows that the results are very similar, which is an indication that within the bandwidth of the laser, the same levels of the C state are populated and give rise to the same dynamics. Figure 5 shows the pump−probe transient dynamics of the $^{16}O^+$ and $^{32}S^+$ species excited with 399.0 nm light. The individual components of the dynamical process deconvoluted by the fitting procedure are depicted with the same graphics as employed in Figure 2. Both ions show the growth and decay dynamics indicative of a reaction product.

The results of a probe laser power study at 397.5 nm are shown in Figure 6 for the $^{16}O^+$ cation. The traces show transient behavior that is a sum of a Gaussian response near the temporal zero and growth/decay dynamics at positive delay times; the transient behavior of S^+ is not shown but is similar to that of O^+. The panels show the change with probe laser power. Lowering the probe power decreases the observed signal until it reaches some threshold and in panel C the pump−probe trace shows only the Gaussian response at the zero; the growth and decay dynamics are absent. Figure 7 shows a quantitative representation of the power study depicted in Figure 6 for S^+ and O^+ at two pump−probe delay times, 0.050 and 0.250 ps. The plotting of the natural log of the signal intensity as a function of the natural log of the laser power gives a slope that is, approximately, the number of photons required to produce the observed signal. The large slopes of the power study plots are indicative of the high probe power dependence of the S^+

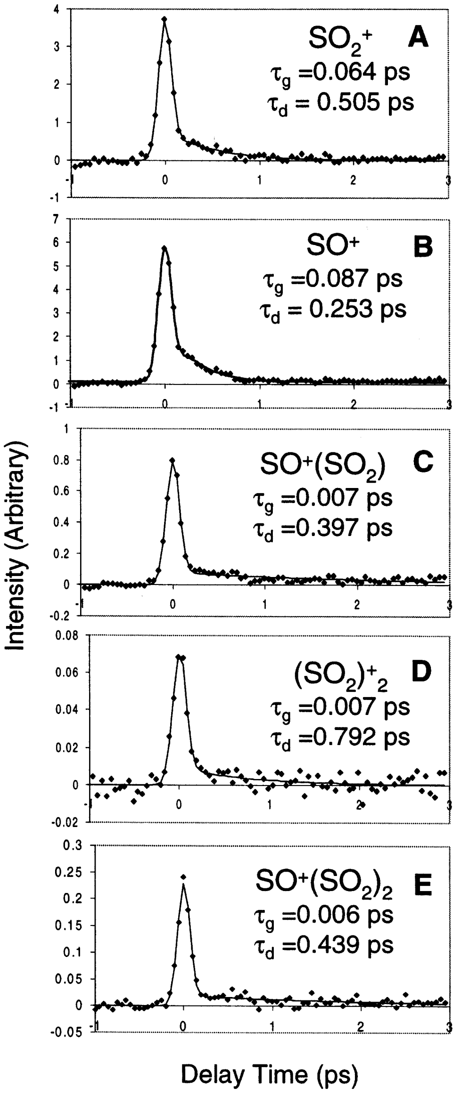

Figure 4. Pump–probe temporal response of SO_2 cluster ions and fragments: (A) SO_2^+ (same data as in Figure 2, shown here again for comparison); (B) SO^+; (C) $SO^+(SO_2)$; (D) $(SO_2)_2^+$; (E) $SO^+(SO_2)_2$. The solid line represents the best fit of data points (squares).The pump wavelength and power are 399.0 nm and 0.22 mJ, respectively. The probe power is 1.0 mJ. The growth time is given by τ_g, and decay time is given by τ_d.

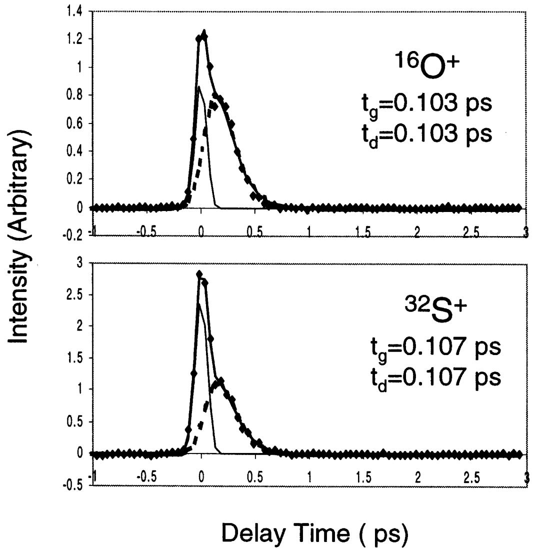

Figure 5. Pump–probe temporal response of $^{16}O^+$ and $^{32}S^+$ at 399.0 nm. The solid line is the best fit of the data points (squares) and is the sum of the thin solid line and the dashed line, which represent the Gaussian response near the zero and the growth (τ_g) and decay (τ_d) dynamics at positive time delays. The pump power is 0.22 mJ, and the probe power is 1.0 mJ.

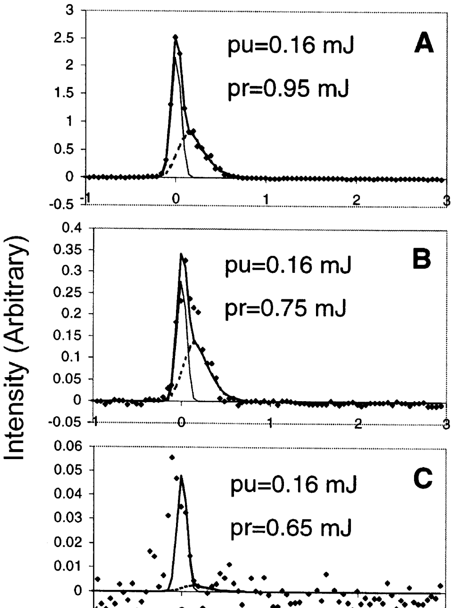

Figure 6. Transient behavior of $^{16}O^+$ showing the power dependence on the probe (pr) laser [(A) 0.95 mJ; (B) 0.75 mJ; (C) 0.65 mJ] with a constant pump power at a pump wavelength 397.5 nm.

and O^+ signal. Figure 8 shows the pump–probe transients of SO_2^+, S^+, and O^+. Note the delay in the observation of S^+ and O^+ relative to that of SO_2^+; the delay was determined in the data fitting procedure to be 0.035 and 0.042 ps for S^+ and O^+, respectively.

Discussion

Our results show that two dissociation pathways are possible in these experiments. As illustrated by the data shown in Figure 2, the transient dynamics of the SO_2^+ shows a Gaussian response near the temporal overlap of the pump and probe beams followed by formation and decay components from the dynamics of the process. One reaction pathway gives rise to the SO_2^+ ion signal at the zero overlap, but a second process must occur to account for the formation of the species at later delay times. Moreover, the mechanism must account for the disappearance of all ion signal at long pump–probe delay times.

The mechanism proposed to account for the observed dynamics is shown in Figure 9. This figure depicts the reaction pathways of an SO_2 cluster that are possible with the wavelengths used in this study. An SO_2 dimer is chosen as an illustrative example, but the mechanism applies to the dimer and larger clusters. In a typical pump–probe scheme, an SO_2 moiety of the dimer is excited to the C state by absorption of two pump photons. At the temporal zero, the pump step is immediately followed by absorption of 4 probe photons to overcome the ionization potential (IP) of the SO_2 molecule (12.34 eV).[15] The effectiveness of multiphoton ionization from the excited C state is clearly evident from the large intensity of $(SO_2)_2^+$ seen at the overlap at zero delay time in Figures 3D and 4D.

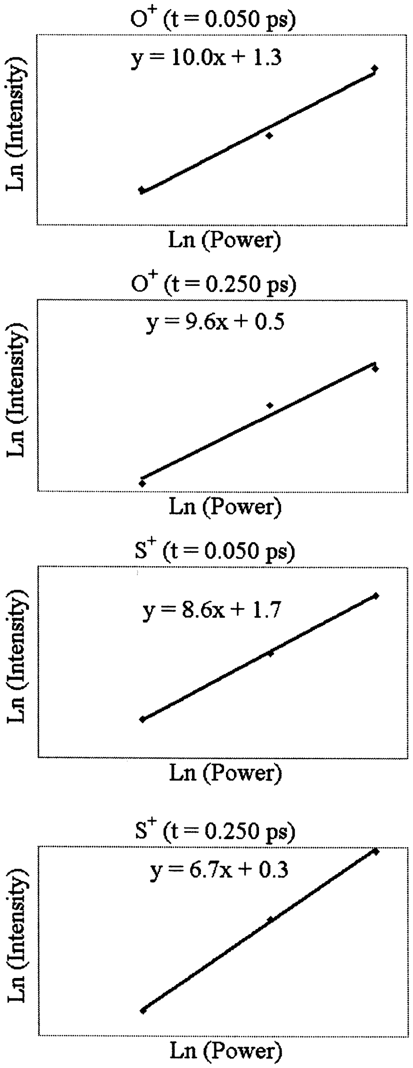

Figure 7. Linear regression plots of the natural log of the signal intensity as a function of the natural log of probe laser power for the $^{16}O^+$ and $^{32}S^+$ signal. The three probe laser powers used are 0.95, 0.75, and 0.65 mJ per pulse with 397.5 nm pump pulse at constant power. Plots are shown for two delay times, which correspond to the two maxima in the $^{16}O^+$ and $^{32}S^+$ signal (see Figure 5).

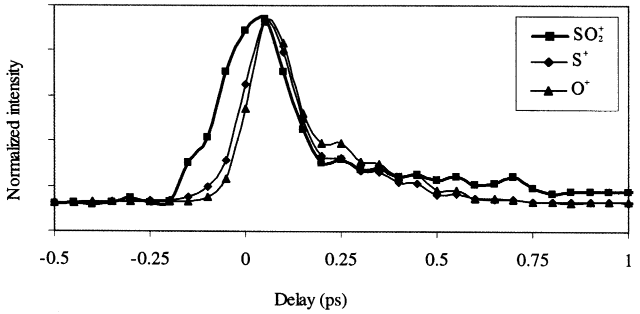

Figure 8. Graphical comparison of $^{16}O^+$ and $^{32}S^+$ temporal behavior to that of SO_2^+. Note the delay of the $^{16}O^+$ and $^{32}S^+$ signal by about 0.040 ps.

At positive pump−probe delay times, the neutral SO_2 dimer is free to move under the influence of the potential energy surface. Dissociation from the C state proceeds through coupling to lower repulsive states.[1,2] The SO_2 dimer can dissociate into (SO + O)(SO_2), as depicted in Figure 9. This would give rise to the decay of the $(SO_2)_2^+$ signal, as seen in Figures 3 and 4. This pathway does not include any formation component in the dynamics. Another pathway is available to the excited dimer; loss of an SO_2 molecule giving rise to SO_2* plus SO_2 (see Figure 9). Because this SO_2* excited species was not present at the temporal zero and formed at some later delay time, the SO_2 temporal response will show a growth component that reflects its formation through the cluster fragmentation pathway. The SO_2* can further dissociate, as shown in Figure 9, which will result in a decrease in the SO_2^+ ion signal and manifest as a decay in the pump−probe transient dynamics.

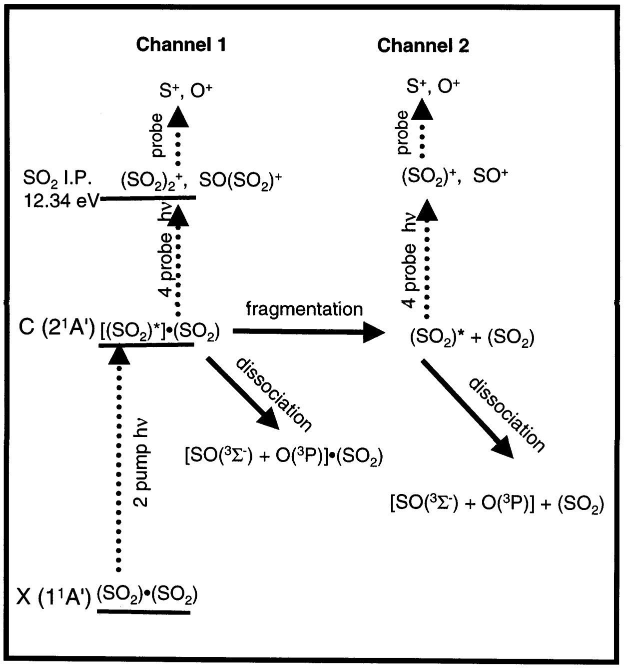

Figure 9. Reaction diagram depicting the proposed mechanism for the dissociation of $(SO_2)_2$, as an example of the cluster dynamics. The first pathway is a simple dissociation of the cluster, and in the second pathway, the cluster first evaporates a cluster molecule, which is followed by dissociation of the chromophore SO_2*.

In the pump−probe temporal response of the clusters (Figures 3 and 4), it was seen that the $SO^+(SO_2)$, $(SO_2)_2^+$, and $SO^+(SO_2)_2$ species did not show a growth component. These species follow a simple exponential decay corresponding to the dissociation of the chromophore of the SO_2 cluster on the C state. Because these species do not form to any appreciable extent by the cluster fragmentation pathway, they should not show the growth component in the dynamics in agreement with the findings presented.

Monomers of SO_2 are present in the molecular beam that do not originate from cluster fragmentation, and these species will also undergo photodissociation. The dynamics of these species cannot be separated from the observed dynamics of SO_2^+ from the cluster fragmentation pathway. However, an SO_2 monomer that does not originate in a cluster will only show decay dynamics indicative of the dissociation into SO + O and will not show growth dynamics. Experiments were conducted on SO_2 in the absence of clusters, confirming that the dynamics of SO_2^+ follows a single-exponential decay with a lifetime of 0.191 ± 0.031 ps when clusters are not present. The transient dynamics did not exhibit any growth components. Thus, in the cluster studies, the measured growth dynamics arise solely from the SO_2 molecules that originate in a cluster and form by the proposed mechanism. One apparent anomalous aspect of the proposed mechanism is the fast growth time of the SO_2^+ (<100 fs, Figures 3A and 4A). Evaporation rates are typically several hundred femtoseconds up to about 1 ps. Therefore, it is necessary to invoke the idea that there is a hot population of the excited clusters that can undergo a fast cluster fragmentation leading to the $(SO_2)^*$. An argument in favor of the concept of a hot population leading to the rapid loss of molecules from the SO_2^* chromophore can be made on the basis of the binding energy of the cluster and the energetics of the C state. In the experiments reported here, a 6.24 eV (2 photons at 397.5 nm) excitation results in the C state having 0.57 eV of excess energy above the crossing to the repulsive 2 $^1A'$ state, which has been found to occur at 5.67 eV.[16] As a result, the 0.57 eV of excess energy must be dissipated from the chromophore molecule before the dissociation process observed in the SO_2 cluster dynamics can occur. The excess energy can leave the chromophore molecule in two ways; the energy can be distributed into the rotational and vibrational modes of the cluster, or the energy can be removed by fragmentation of the cluster with the excess energy going into overcoming the binding energy of the cluster (about 0.1 eV/molecule)[17] and into translational energy of the lost molecules. It seems reasonable to assume that both of these processes occur within the cluster population. Because the SO_2 molecules within the cluster are not identical and a number of possible cluster structures exist,[17] the orientation of the chromophore molecule relative to the other molecules in the cluster will vary. The orientation of the chromophore within the cluster is expected to determine which energy loss pathway will occur in that particular cluster. As a result, a portion of the cluster population will undergo energy redistribution; these clusters will be observed in the mass spectrum and follow the mechanism described by channel 1 of Figure 9. Alternatively, some cluster will undergo fragmentation; these clusters will never be observed in the mass spectrum, but products will be observed as depicted by channel 2 of Figure 9.

From the C state, the SO_2 monomer can dissociate into SO ($^3\Sigma^-$) and O (^3P) (mechanism shown on the lower part of Figure 9), where both of these species are produced in the electronic ground state. If SO and O were ionized by the probe beam alone, their pump−probe traces would show a long lifetime, because these are the end products of the photodissociation. As seen in Figures 3−5, the SO^+ and O^+ are not long-lived. This shows that the SO^+ and O^+ observed in the mass spectra do not arise from the ionization of the neutral dissociation products. In addition, ionization of neutral dissociation products does not account for the appearance of S^+ in the mass spectrum because S is not a neutral dissociation product of the C state.

Predissociation of the ground-state SO_2^+ ion is known to occur,[18] which gives rise to the SO^+ and $(SO_2)_nSO^+$ signal. Predissociation is the dominant ion state cluster reaction product as can be seen in the mass spectrum shown in Figure 1. As discussed earlier, S^+ and O^+ cannot result from the ionization of neutral dissociation products; thus, O^+ and S^+ must originate from fragmentation in the ion state. In a nanosecond REMPI study of SO_2, the ions S^+ and O^+ were seen in the mass spectra, and the authors attributed this observation to the photodissociation of SO^+ in an excited ion state.[19] This is depicted in Figure 9 as a pathway involving the absorption of further probe photons above the ionization potential. It has been determined by electron-impact ionization[20] that the formation of S^+ and O^+ from SO requires excitation of SO to 5.6 eV (S^+) and 11.9 eV (O^+) above the ionization potential of SO. Because the ionization event in the experiment reported here occurs from the excited SO_2^* C state (6.24 eV) and not the ion state, a comparison to the results of ref 20 requires consideration of the additional energy needed to reach the ionization potential of SO (10.29 eV)[21] from the C state. Using the above line of reasoning, S^+ and O^+ formation from probing of the C state excited SO_2^* and its clusters should require about 9.65 and 15.95 eV, respectively. This corresponds to 7 photons of the 795 nm probe to produce S^+ and 11 photons of the probe to produce O^+. These values agree very well with the results of the power study plots shown in Figure 7, which indicate the absorption of 7 to 8 probe photons to produce the S^+ signal and 9 to 10 photons to produce O^+.

As mentioned earlier, the dynamics of the S^+ and O^+ signal show a large Gaussian-shaped signal at zero time delay followed by fast growth and decay dynamics. As seen in Figure 8, the Gaussian part of the S^+ and O^+ signals appear about 0.040 ps after that of the SO_2^+. It appears that because the formation of S^+ and O^+ requires absorption of a large number of photons, S^+ and O^+ can only be observed when SO_2^* and its clusters are in a Franck−Condon region that is resonant with the excited ion state. It can be seen in the bond angle and bond length potential energy surface of SO_2[2] that the structure of the excited-state SO_2 molecule differs slightly from that of the ground-state molecule. As a result, the 0.040 ps delay of the S^+ and O^+ signal must be the result of the vertically excited SO_2 clusters evolving into the excited-state geometry and thus into the Franck−Condon region, allowing the multiphoton absorption necessary for the production of S^+ and O^+. However, because the SO_2 clusters are traveling rapidly on the excited-state surface, they move out of the Franck−Condon region within the pulse width of the laser. The rise and decay in the S^+ and O^+ signal centered at 0.250 ps is thought to be the result of a process similar to the one descried above except the appearance of the S^+ and O^+ is delayed by the cluster fragmentation process depicted in Figure 9. One would expect the cluster fragmentation process to have a cluster size dependence; unfortunately, because the process is so rapid, the small difference between the temporal response of S^+ and O^+ produced from various cluster sizes cannot be resolved.

Conclusions

In these studies, it has been shown that dissociation from the neutral C state involves multiple pathways when clusters of SO_2 are excited. A mechanism of dissociation of SO_2 clusters has been proposed to account for the observations. The excited SO_2 cluster can simply dissociate from the C state, or it can first loose cluster molecules, giving rise to a growth term in the dynamics followed by an exponential decay. It was observed that the dynamics of $(SO_2)_nSO^+$ clusters reflect those of $(SO_2)_{n+1}^+$ clusters due to the ion state loss of oxygen atoms through ion state predissociation. It was also concluded that S^+ and O^+ signals are the product of an ion excited state process that is only operative when the resonant multiphoton absorption conditions of the Franck−Condon region are present.

Acknowledgment. Financial support by the Atmospheric Sciences Division and Experimental Physical Chemistry Division of the U.S. National Science Foundation, Grant No. NSF-0089233, is gratefully acknowledged.

References and Notes

(1) Ray, P. C.; Ardent, M. F.; Butler, L. J. *J. Chem. Phys.* **1998**, *109*, 5221.

(2) Katagiri, H.; Sako, T.; Hishikawa, A.; Yazaki, T.; Onda, K.; Yamanouchi, K.; Yoshino, K. J. *Mol. Struct.* **1997**, *589*, 413.

(3) Sato, T.; Kinugawa, T.; Arikawa, T. *Chem. Phys.* **1992**, *165*, 173.

(4) Nachtigall, P.; Hrušák, J.; Bludský, O.; Iwata, S. *Chem. Phys. Lett.* **1999**, *303*, 441.

(5) Wisniewski, E. S.; Castleman, A. W., Jr. *J. Phys. Chem. A* **2002**, *106*, 10843.

(6) Snodgrass, J. T.; Bunn, T. L.; Bowers, M. T. *Int. J. Mass. Spectrom. Ion Processes* **1990**, *102*, 45.

(7) Erickson, J.; Ng, C. J. *J. Chem. Phys*. **1981**, *75*, 1650.

(8) Zhong, Q.; Hurley, S. M.; Castleman, A. W., Jr. *Int. J. Mass. Spectrom. Ion. Processes* **1999**, *185/186/187*, 905.

(9) Rose, T. S.; Rosker, M. J.; Zewail, A. H. *J. Chem. Phys.* **1989**, *91*, 7415.

(10) Shi, Z.; Ford, J. V.; Wei, S., Castleman, A. W., Jr. *J. Chem. Phys*. **1993**, *99*, 8009.

(11) Breem, J. J.; Kilgore, K.; Tzeng, W.-B.; Wei, S.; Keesee, R. G.; Castleman, A. W., Jr. *J. Chem. Phys*. **1989**, *90*, 11.

(12) Zhong, Q.; Poth, L.; Shi, Z.; Ford. J. V.; Castleman, A. W., Jr. *J. Phys. Chem. B* **1997**, *101*, 4203.

(13) Snyder, E. M.; Purnell, J.; Wei, S.; Buzza, S. A.; Castleman, A. W., Jr. *Chem. Phys*. **1996**, *207*, 355.

(14) Wisniewski, E. S. Doctoral Dissertation, The Pennsylvania State University, 2002.

(15) Wang, L.; Lee, Y. T.; Shirley, D. A. *J. Chem. Phys*. **1987**, *87*, 2489.

(16) Becker, S.; Braatz, C.; Lindner, J.; Tiemann, E. *Chem. Phys.* **1995**, *196*, 275.

(17) Bone, R. G. B.; Le Sueur C. R.; Amos R. D.; Stone, A. J. *J. Chem. Phys.* **1992**, *96*, 8390.

(18) Thomas, T. F.; Dale, F.; Paulson, J. F. *J. Chem. Phys*. **1986**, *84*, 1215.

(19) Zhang, L.; Pei, L.; Dai, J.; Zhang, T.; Chen, C.; Yu, S.; Ma, X. *Chem. Phys. Lett*. **1996**, *259*, 403.

(20) Tarnovsky, V.; Levin, A.; Deutsch, H.; Becker, K. *J. Chem. Phys.* **1995**, *102*, 770.

(21) Norwood, K.; Ng, C. Y. *Chem. Phys. Lett.* **1998**, *156*, 145.